Inhibition of small Maf function in pancreatic beta cells improves glucose tolerance through the enhancement of insulin gene transcription and insulin secretion

Hiroshi Nomoto,[1] Takuma Kondo,[1] Hideaki Miyoshi,[1] Akinobu Nakamura,[1] Yoko Hida,[1] Ken-ichiro Yamashita,[2] Arun J. Sharma,[3,4] and Tatsuya Atsumi[1]

[1] Division of Rheumatology, Endocrinology and Nephrology, Hokkaido University Graduate School of Medicine, Sapporo, Japan

[2] Department of Transplant Surgery, Hokkaido University School of Medicine, Sapporo, Japan

[3] Section of Islet Transplantation and Cell Biology, Joslin Diabetes Center, Boston, Massachusetts, USA

[4] MedImmune LLC, Gaithersburg, Maryland, USA

***Abbreviated Title*:** Roles of small Maf factors in beta cells

***Key terms*:** small-Maf factors, transcriptional factors, pancreatic beta cell, insulin transcription

***Word count*:** 4077 words

***Number of figures and tables*:** 7

***Corresponding author and person to whom reprint requests should be addressed*:**

Takuma Kondo, MD, PhD

Division of Rheumatology, Endocrinology and Nephrology, Hokkaido University Graduate School of Medicine, North 15, West 7, Kita-ku, Sapporo, Hokkaido 060-8638, Japan

Telephone: +81-11-706-5915

Fax: +81-11-706-7710

E-mail: takkondo@med.hokudai.ac.jp

Disclosure Statement: The authors have nothing to disclose.

ABSTRACT

The large-Maf transcription factor MafA has been found to be crucial for insulin transcription and synthesis and for pancreatic β-cell function and maturation. However, insights about the effects of small Maf factors on β-cells are limited. Our goal was to elucidate the function of small-Maf factors on β-cells using an animal model of endogenous small-Maf dysfunction. Transgenic (Tg) mice with β-cell–specific expression of dominant-negative MafK (DN-MafK experiments), which can suppress the function of all endogenous small-Mafs, were fed a high-fat diet (HFD) and their *in vivo* phenotypes were evaluated. Phenotypic analysis, glucose tolerance tests, morphologic examination of β-cells, and islet experiments were performed. DN-MafK–expressed MIN6 cells were also used for *in vitro* analysis. The results showed that DN-MafK expression inhibited endogenous small-Maf binding to insulin promoter while increasing MafA binding. DN-MafK Tg mice under HFD conditions showed improved glucose metabolism compared with control mice via incremental insulin secretion, without causing changes in insulin sensitivity or MafA expression. Moreover, upregulation of insulin and glucokinase gene expression was observed both *in vivo* and *in vitro* under DN-MafK expression. We concluded that endogenous small-Maf factors negatively regulates β-cell function by competing for MafA-binding and thus the inhibition of small-Maf activity can improve β-cell function.

INTRODUCTION

Although various factors affect the transcription, synthesis and secretion of insulin in pancreatic islet beta cells, some pancreatic transcriptional factors such as Pancreatic and duodenal homeobox factor 1 (Pdx-1), Neurogenic differentiation factor 1 (NeuroD1) and v-maf musculoaponeurotic fibrosarcoma oncogene homolog A (MafA) have been certified to be intimately involved in insulin transcription under the conditions of glucolipotoxicity (1-4). These transcriptional factors bind to conserved enhancer elements in the promoter region of the insulin genes, and regulate glucose-responsive insulin gene transcription and, consequently, insulin secretion and synthesis. Pdx-1 and MafA are selectively expressed in pancreatic beta cells, whereas NeuroD1 is expressed in all pancreatic endocrine cells. All 3 factors are involved in both insulin gene expression and islet and pancreas development and maturation (5,6).

In particular, the transcription factor MafA has been reported to be a key regulator of insulin gene transcription and beta cell maturation (7-11). Maf transcription factors belong to the basic leucine zipper (bZIP) family, and the Maf family is divided into 2 groups, large-Maf factors and small-Maf factors. Large-Maf factors include MafA, c-Maf, MafB, and neural retina-specific leucine zipper protein (NRL) (12,13). Large-Mafs possess a DNA-binding domain and an N-terminal transactivating domain; therefore, they play key roles in gene regulation and transcription.

On the other hand, small-Maf transcription factors, including MafF, MafG, and MafK, are expressed in a wide variety of tissues at various levels (14-16). Although small-Maf factors lack a transactivation domain, they act as transcriptional regulators by binding to a DNA sequence known as the Maf recognition element (MARE) (17). Small-Maf factors form heterodimers with the CNC family of proteins, including Nrf1, Nrf2, Nrf3, Bach1, and Bach2, which further interact with Fos and FosB, but not with large-Maf factors (17-19). Homodimer of small-Maf factors suppress transcriptional activity of large-Maf factors via MARE, but small-Maf heterodimers can act as either suppressors or activators depending on their dimerization partners (17). It has been reported that MafK expression inhibited insulin transcription competing with MafA, moreover, in pancreatic islets, beta cell specific overexpression of MafK was reported to result in the impairment of

glucose-stimulated insulin secretion only at a young age and resulted in reciprocal islet hypertrophy and compensatory increase in the DNA-binding activity of MafA in adult age (20).

However, little is known about the function of endogenous small Maf factors in pancreatic beta cells *in vivo*, and the association between small-Maf factors and the diabetic state is also not well understood. To clarify the role of small-Maf factors *in vivo*, we aimed to repress endogenous small-Maf functions using dominant-negative MafK (DN-MafK), which lacks the part of the DNA-binding domain of endogenous MafK that reportedly decreases NF-E2 DNA-binding activity (21). In this report, we describe the generation of pancreatic beta cell–specific DN-MafK transgenic (Tg) mice and characterize their metabolic phenotype.

RESEARCH DESIGN AND METHODS

Generation of transgenic mice

Construction of the expression vector, including the 1.9-KB human insulin promoter used to generate transgenic mice, has been described previously (22). The vector was provided by Dr. Yamaoka (Institute for Genome Research, University of Tokushima, Tokushima, Japan). The DN-MafK mutant construct described elsewhere (21) was provided by Dr. Orkin (Children's Hospital, Boston, MA, USA). This DN-MafK construct was inserted into the multiple cloning sites in the cytomegalovirus (CMV) expression vector with N-terminal 3 tandem Flag tags (Sigma-Aldrich, St. Louis, MO, USA). Flag-DN-MafK was subcloned into the cloning site flanking the exon–intron organization and a polyadenylation signal of the rabbit β-globin gene. The BssHII-excised fragment of this vector, excluding the plasmid-derived sequence, was used as the transgene. Integration of the transgene into the mouse genome was detected by PCR, between a sense primer in exon 1 of the human insulin promoter (5′-GCATCAGAAGAGGCCATCAA-3′) and an antisense primer in exon 3 of the rabbit β-globin gene (5′-ACTCACCCTGAAGTTCTCAG-3′), and by Southern blot analysis. The *Sal*I–*Not*I fragment of the transgene was used as a probe and compared with indicator bands of 1, 10, and 100 copies of the transgene. Three lines of Tg mice (No. 72, 23, and 53) were established on the C57BL/6J background.

Animal care and diet

All mice were housed at 2–4 animals per cage under controlled ambient conditions and a 12:12 h light/dark cycle, with lights on at 07:00 h. The animals were maintained in accordance with standard animal care procedures based on the institutional guidelines at Hokkaido University Graduate School of Medicine and were given free access to drinking water and diet. Both wild-type (Wt) and DN-MafK Tg male mice were fed standard chow (Oriental Yeast, Tokyo, Japan) until 5 (Fig. 1 and Supplementary Fig. 1) or 6 (Figs. 3, 4, 5, 6, 7 and Supplementary Fig. 3 and 4) weeks of age and were subsequently switched to a high-fat diet (HFD) for 10 (Figs. 3, 4, 5, 6, 7 and Supplementary Fig. 3 and 4), 14 (Fig. 2) or 15 (Fig. 1 and Supplementary Fig. 1) weeks, and an additional 10 weeks

(Supplementary Fig. 1). The HFD contains 56.7% calories from fat and 20.1% calories from protein (High Fat Diet 32, Clea Tokyo, Tokyo, Japan).

Measurement of biochemical markers

Body weight was monitored weekly from 6 weeks of age, and a random blood glucose test was performed every 2 weeks using a One Touch Ultra blood glucose meter (Johnson & Johnson, New Brunswick, NJ, USA). Blood samples were also collected from the tail vein every 2 weeks. For glucose tolerance testing, the plasma was separated and stored at −80°C until use for insulin measurement. The concentration of insulin in the plasma was measured using an enzyme-linked immunosorbent assay (ELISA) kit (Morinaga Institute of Biological Science, Yokohama, Japan).

Intraperitoneal and oral glucose tolerance testing

All mice underwent the oral glucose tolerance test (OGTT) at 16 weeks of age or the intraperitoneal glucose tolerance test (ipGTT) at 20 weeks of age**.** After a 16 h overnight fast, the mice were intraperitoneally or orally loaded with glucose at a concentration of 1.0 mg/g body weight. We obtained blood samples at 0, 15, 30, 60, 90, and 120 min after glucose loading. Glucose and plasma insulin levels were measured as described above.

Insulin tolerance testing

After the mice were given free access to diet, human insulin (Humalin R; Eli Lilly, Indianapolis, IN, USA) was injected intraperitoneally at a concentration of 0.75 mU/g body weight at 16 weeks of age. Blood samples were collected from the tail vein every 30 min, and blood glucose was determined immediately as described above.

Immunohistochemical analysis

Isolated pancreatic tissues were immersion-fixed in 4% formalin at 4°C overnight. Tissues were then roughly paraffin-embedded, and 5-μm sections were mounted on glass slides. Sections were immersed

for 15 min in methanol containing 0.3% (v/v) hydrogen peroxide to deactivate endogenous peroxidase activity. After rinsing with PBS, the sections were immunostained with a specific antibody, including rabbit anti-human insulin (diluted 1:1000), anti-MafF/G/K (1:200), and anti-Flag (1:1000) antibodies (Santa Cruz Biotechnology, Dallas, TX, USA). The sections were counterstained with hematoxylin.

For fluoroimmunostaining, tissue sections were incubated overnight at 4°C with rabbit anti-human insulin (1:1000), anti-Maf F/G/K (1:200) (Santa Cruz), anti-mouse insulin monoclonal antibody (1:1000), anti-Flag (1:1000) (Sigma-Aldrich), and anti-proliferative cell nuclear antigen (PCNA) monoclonal antibody (Nichirei, Tokyo, Japan). After rinsing with PBS, Alexa 488 goat anti-mouse antibody and Alexa 594 donkey anti-goat antibody (Invitrogen, Carlsbad, CA, USA) were added, and the mixture was incubated for 30 min. To estimate β-cell mass, the area of insulin-positive cells was measured with BZ-II analyzer (Keyence, Osaka, Japan) according to the manufacturer's instructions, and β-cell mass was calculated by the following formula: β-cell mass (mg) = the pancreas weight (mg) × percent pancreatic islet area × percent β-cell count. PCNA-positive β-cells were counted separately from insulin-positive islet cells.

Islet isolation

Islets were isolated using collagenase XI (Sigma-Aldrich) according to the manufacturer's instructions, as described elsewhere (23,24).

Glucose-stimulated insulin secretion

Insulin secretion was measured after culturing islets from Wt and DN-MafK Tg mice for 4 h in RPMI-1640 medium containing 11 mM glucose supplemented with 10% FBS and 1% penicillin–streptomycin (Sigma-Aldrich). Size-matching five islets were preincubated at 37°C for 30 min in Krebs–Ringer bicarbonate HEPES (KRBH) buffer containing 2.8 mM glucose, followed by incubation with 2.8, 5.6 or 11.2 mM glucose solution for 90 min. The isolated islets were extracted in acid-ethanol, and their insulin content was measured. Insulin was immunoassayed as described above.

Construction of adenovirus-DN-MafK

An adenovirus vector containing DN-MafK and green fluorescent protein (GFP) genes was constructed with the help of O.D. 260 Inc. (Boise, ID, USA). Briefly, DN-MafK cDNA along with rabbit β-globin polyA was cloned into a pE1.2 shuttle plasmid, and a GFP fragment along with rabbit β-globin polyA was inserted into a pE3.1 shuttle plasmid. These plasmids were then further modified as described previously (25). Adenovirus that possessed the CMV-GFP expression cassette in the E1 region of the virus genome was used as a control virus (O.D. 260 Inc.). The adenovirus titer was determined using the OD 260-SDS method as described previously (25).

Cell culture and transduction

Cells from the MIN6 cell line (passage 43–50) were grown in Dulbecco's modified Eagle medium (DMEM) containing 15% FBS or in glucose-free DMEM (Invitrogen) containing 10% dialyzed FBS (Invitrogen) and 1% penicillin–streptomycin with the indicated concentration of glucose (Sigma Chemical Co, St. Louis, MO, USA). The cells were then transduced with Ad-DN-MafK or Ad-GFP at multiplicity of infection of roughly 20. They were incubated for 2 h, followed by washing and further culturing for 48–60 h. Efficacy of infection was confirmed by fluorescence microscopy, and confirmation of flag-DN-MafK expression was performed by Western blotting using anti-Flag antibody. The collected cells were used for protein and RNA extraction.

Luciferase assay

The insulin promoter lesion (-238 to 0 bp) containing plasmid and the reporter plasmid were generated. The Flag-DN-MafK cDNA was subcloned into the pcDNA 3.1 vector and these plasmids were transfected into Ad-GFP or Ad-DN-MafK infected MIN6 cells using Lipofectamine™ 2000 (Invitrogen). pcDNA plasmid was used to adjust the dose of DNA. Dual-Luciferase® reporter assays were performed 48 h after transfection according to manufacturer's protocol (Promega), then absorbance was measured using Glomax® Luminometer (Promega). The firefly luciferase data normalized by Renilla was used for analysis.

Immunoblot analysis

Frozen tissues or collected cells were lysed in erythrocyte lysis buffer [ELB; 50 mM HEPES, pH 7.0, 250 mM NaCl, 0.1% Nonidet P-40, 5 mM EDTA, 0.5 mM dithiothreitol supplemented with 1 mM phenylmethylsulfonyl fluoride (PMSF), 1 μg/mL leupeptin, 1 μg/mL aprotinin, 50 mM sodium fluoride, and 0.2 mM sodium orthovanadate] containing benzamidine and beta-glycerophosphate. Lysates were sonicated twice on ice and cleared by centrifugation. The protein content of the whole cell extract was measured by NanoDrop (LMS, Tokyo, Japan). Equal amounts (20 μg) of proteins were separated on 10% SDS-polyacrylamide gel and transferred to a nitrocellulose membrane. The primary antibodies used were anti-MafF/G/K (1:2000), anti-Actin (1:2000), and anti-Flag for detecting Flag-DN-MafK (1:2000) antibodies. Anti-Actin antibody was used as a loading control. The secondary antibodies were anti-rabbit IgG (MafF/G/K), anti-goat IgG (Actin), or anti-mouse IgG (Flag). Analysis was performed using Amersham ECL Advance Western blotting detection kit (GE Healthcare, Little Chalfont, Buckinghamshire, UK), and images were obtained using the CCD-camera system LAS-4000 UV mini (Fujifilm, Tokyo, Japan).

Chromatin immunoprecipitation assay

Chromatin immunoprecipitation (ChIP) analysis was performed using a ChIP assay kit (EMD Millipore, Billerica, MA, USA). Adenovirus-infected MIN6 cells were preincubated in a 10-cm dish for 48 h. The cells were formaldehyde cross-linked for 10 min, following which they were washed and collected with PBS-containing protease inhibitors (50 μg/mL PMSF, 10 μg/mL aprotinin, and 10 μg/mL leupeptin). The cells were suspended in SDS lysis buffer and sonicated 5 times to obtain 200–1000 base-pair fragments. Immunoprecipitation was performed using Sperm DNA/Protein A agarose slurry. 2 μg of the following antibodies were used for immunoprecipitation: anti-rabbit MafA (Bethyl, Montgomery, TX, USA), anti-rabbit Maf F/G/K (Santa Cruz), and normal rabbit IgG (Santa Cruz). Washing and chromatin elution were performed according to the manufacturer's instructions. Primers for the insulin promoter were TAATTACCCTAGGACTAAGTAGAGGTGTTG (forward) and

AGGTGGGGTAGGTCAGCAGATGGCCAGA (reverse). 30 cycles were performed for PCR analysis. Quantitation of band density is performed using an imaging densitometer and normalized to the band density of control MIN6 cells.

RNA isolation and real-time PCR

Total RNA was isolated from the isolated islets and Ad-infected MIN6 cells using the RNeasy Mini Kit (Qiagen, Hilden, Germany) according to the manufacturer's recommendation and was used as the starting material for cDNA preparation. A real-time PCR study was performed in duplicate on a 7500 Fast Real Time PCR system using SYBR Green PCR Master Mix (Applied Biosystems, Santa Clara, CA, USA). The results were quantified using the ΔΔCT method, and the expression was normalized to glyceraldehyde 3-phosphate dehydrogenase (GAPDH).

Statistical analysis

Results are expressed as mean ± standard error (SE). Differences between the 2 groups were assessed using Student's *t* tests. Individual comparisons between more than 2 groups were analyzed by ANOVA. A p-value of <0.05 was considered statistically significant. Data were analyzed using Ekuseru–Toukei 2012 (Social Survey Research Information, Tokyo, Japan).

RESULTS

Expression of small-Maf factors in the pancreatic islets of mice fed an HFD

The role of endogenous small Maf factors in regulating pancreatic beta cell function is unknown. Therefore, we first confirmed the expression pattern of small Maf factors in islets. Pancreatic islets were isolated from 2 groups of C57BL/6J mice at 12 weeks of age, after feeding the animals either a normal diet (ND) or an HFD from 5 weeks of age. Whole cell extracts were prepared and analysed by Western blotting. Small Maf expression levels were significantly higher in the islets of the HFD-fed mice than in those of the ND-fed mice (Fig. 1A). Pancreatic sections immunostained with insulin and small-Maf-specific antibody showed the expected increase in the islet size in the HFD-fed mice than in the ND-fed mice (Fig. 1B). Furthermore, small Maf proteins were expressed and relatively highly observed in the nuclei of the beta cells in the islets (Fig. 1C). These data show that the expression of small-Maf factors in pancreatic beta cells is enhanced in HFD-fed mice.

Specific inhibition of small Maf factors in pancreatic β-cells

Despite the increased small Maf expression in beta cells, serum insulin levels remained higher in HFD-fed mice than in ND-fed mice, as did blood glucose levels (Fig. 1A and Supplementary Fig. 1), consistent with compensatory response to the insulin resistance. This finding also indicates that relatively impaired beta cell function during the compensatory phase may be associated with enhanced small Maf expression, therefore, the inhibition of small Maf function may overcome beta cell dysfunction. To test this hypothesis, we used the Flag-DN-MafK transgene as a negative regulator of endogenous small-Maf functions and prepared the Ad-DN-MafK infected MIN6 cells and DN-MafK Tg mice. In regards to Ad-infected MIN6, efficacy of infection was equivalent to control MIN6 cells (Fig. 2A) and abundant DN-MafK protein expression was confirmed (Fig. 2B). Because DN-MafK lacking a basic region in the DNA-binding domain (Fig. 3A) didn't bind to MARE on insulin-2 promoter region (Supplementary Fig. 2), DN-MafK can theoretically inhibit the function of all small Maf proteins, including MafF, MafG, and MafK. Indeed, our ChIP assay results suggested the repression of insulin promoter binding of endogenous small-Maf in the DN-MafK–expressed

MIN6 cells compared with that in the control cells, whereas MafA binding to MARE was significantly increased (Fig. 3B). Furthermore, luciferase assay using insulin promoter resulted in significant increment of insulin transcriptional activity in DN-MafK expression (Fig. 3C).

All 3 lines of DN-MafK Tg mice (No. 72, 23, and 53) showed normal size and growth (data not shown). We checked the copy numbers of integrated transgene for each line using Southern blotting (Fig. 4A). All lines showed between 1–10 copies of transgene integration, and all had similar phonotypes. The line 53, which showed the most copies, was used for the later experiment. Next, we checked DN-MafK expression in various tissues. Western blot analysis using extracts from various tissues showed that DN-MafK was expressed only in the pancreas (Fig. 4B). Moreover, immunohistochemistry data using anti-Flag tag antibodies demonstrated that DN-MafK was exclusively expressed in islet cells (Fig. 4C).

After feeding both Wt and Tg male mice either the ND or the HFD from 6 weeks of age, ipGTT was performed at 20 weeks of age. Among the ND-fed mice, there were no significant differences in glucose tolerance between the Wt and DN-MafK Tg groups (Fig. 4D). However, glucose tolerance in the HFD-fed Tg mice was significantly improved compared with that in the HFD-fed Wt mice (Fig. 4D and 4E, white circles and white squares). We isolated islets from these mice and performed Western blot analyses. The results demonstrated that MafA protein expression in the islets was slightly increased in the Wt and Tg HFD-fed mice compared with that in both groups of ND-fed mice. However, similar MafA expression levels were observed in both groups of HFD-fed mice (Fig. 4F).

Phenotypic analysis of HFD-fed DN-MafK Tg mice

Because glucose tolerance was significantly improved in the HFD-fed Tg mice compared with that in the Wt mice, further phenotypic analyses were performed to clarify the factors affecting this improvement. There were no significant differences in body weight, food intake, and insulin sensitivity between the Wt and DN-MafK Tg mice (Fig. 5A, 5C and Supplemental Fig. 3). Nonetheless, at 16 weeks of age, a significant improvement in random blood glucose levels (Fig. 5B)

and area under the curve for OGTT results was observed in the DN-MafK Tg mice compared with that in the Wt mice (Fig. 5D and 5E). Moreover, both fasting and post-glucose loaded serum insulin levels were significantly increased in the HFD-fed DN-MafK Tg mice (Fig. 5F). Because impairment in *in vivo* glucose stimulated insulin secretion was ameliorated in the HFD-fed DN-MafK Tg mice while their insulin sensitivity remained unchanged, we postulate that the dysfunction in glucose-responsive insulin-secretion machinery in beta cells may be rectified in these Tg mice.

Islet morphology in the HFD-fed Wt mice and DN-MafK Tg mice

Some previous studies have reported changes in the morphology of pancreatic islets in conjunction with pancreas-specific knockout or overexpression of Maf factors (11,26). In consideration of these findings, we next performed immunostaining of pancreatic sections with antibody against insulin and PCNA to investigate the islet morphology in the HFD-fed mice. Insulin-positive pancreatic cell mass was calculated as described earlier. There were no obvious changes in the morphology of islets (Supplemental Fig. 4A) or the amount of pancreatic beta cells (Supplemental Fig. 4B). Double fluorescence staining with anti-PCNA and anti-insulin antibody indicated that the proliferation of beta cells was also the same in the HFD-fed Wt and DN-MafK Tg mice (Supplemental Fig. 4C and 4D).

Insulin secretion and gene expression of insulin and glucokinase

To evaluate changes in islet function and gene profiling in DN-MafK Tg animals, we performed glucose-stimulated insulin secretion (GSIS) and real-time reverse transcriptase-PCR on RNA from pancreatic islets isolated from the HFD-fed Wt and DN-MafK Tg mice. The GSIS results showed enhanced insulin secretion from the DN-MafK Tg than the Wt islets at all glucose concentrations; the insulin content of islets was also higher in the DN-MafK Tg mice (Fig. 6A, 6B and 6C). Moreover, DN-MafK Tg mice showed a significant increase in the expression of Insulin-1, Insulin-2 and glucokinase genes (Fig. 7A). On the other hand, the expression levels of *Mafa* and *Glut2* were similar in both groups. DN-MafK expressing MIN6 cells also showed significantly higher levels of insulin-1 and insulin-2 gene expression as well as increase in glucokinase gene expression compared with the

316 control MIN6 cells (Fig. 7B). These results suggest that the inhibition of small-Maf function causes an
317 increase in insulin-1 and insulin-2 gene expressions independent of *Mafa* expression, possibly in part
318 via alterations in glucose metabolism resulting from increased *glucokinase* expression in the islets of
319 the HFD-fed Tg mice.
320
321 **DISCUSSION**
322 From this study, we were able to draw 2 major conclusions. First, the inhibition of endogenous
323 small-Maf function using DN-MafK may alter the binding activity of other transcriptional factors,
324 including MafA. Small-Maf factors are known to heterodimerize with the CNC transcriptional family.
325 However, when they form homodimers, they may function as competitive inhibitory factors for
326 MARE binding and would compete with MafA for binding to these sites (20). A heterodimer of
327 endogenous small-Maf and dominant-negative small-Maf with mutations in the DNA-binding domain
328 will suppress the DNA-binding ability of the endogenous small-Maf partner. Importantly, as the
329 small-Maf factors do not form heterodimers with large-Maf factors, DN-MafK will not directly affect
330 the binding and function of large-Maf factors. In a previous study, beta cell–specific overexpression of
331 MafK was found to result in compensatory enhancement of MafA binding (20). Our results suggest
332 that a similar underlying mechanism may exist in our study. Moreover, MAFA expression levels in
333 islets were similar between HFD-fed Wt and DN-MafK Tg mice (Fig. 2G). This may represent a
334 compensatory mechanism for beta cells to adapt to a higher insulin demand. Furthermore, the
335 comparable expression of MAFA in both groups of HFD-fed mice suggest that the amelioration of
336 glucose tolerance in HFD-fed Tg mice likely results from the inhibition of small-Maf function, not
337 from the enhancement of MAFA expression in the beta cells. One possibility is that due to the
338 competition between these transcriptional factors for MARE binding, DN-MafK transgenic islets may
339 have relatively higher proportion of MafA bind to the MARE.
340 Second, inhibition of small-Maf function resulted in significantly increased insulin secretion
341 via the enhanced expression of insulin-1 and insulin-2 genes from pancreatic islets. This finding may
342 be partially explained by the elevation of MafA binding to MARE on insulin promoters, as described

above. Such an indirect increase in the binding of MafA to insulin MARE elements will lead to the induction of insulin gene transcription. Moreover, there is a possibility that DN-MafK directly enhances insulin gene expression by inhibiting the repressive effects of endogenous small-Maf factors. It is important to note that this increase in insulin gene expression occur independent of any increase in *Mafa* mRNA expression and MafA protein level. Another possibility is that incremental *Glucokinase* expression in the islet of DN-MafK Tg mice may in part affect the insulin gene expression. Glucokinase is the rate-limiting enzyme of the glycolytic pathway (27), and it acts as a glucose sensor for glucose-stimulated insulin secretion in the pancreas (28,29). Moreover, it was reported that glucokinase activation actually increases pancreatic beta cell proliferation (30), and in HFD-fed mice, haploinsufficiency of beta cell–specific glucokinase resulted in impaired beta cell mass and function (31). Some previous studies showed that the overexpression of MafA or PDX-1 in pancreatic islets and beta cell lines similarly resulted in the upregulation of glucokinase mRNA expression (32,33), and NeuroD1 was also proposed to regulate pancreatic glucokinase activity (34). In addition, MafA is known as a positive regulator of Pdx-1 and NeuroD1 (11,32). In our study, the upregulation of MafA binding may have partially resulted in glucokinase expression. Because of the inhibition of small-Maf factors, similar to the effect of glucokinase activation, fasting plasma insulin levels and GSIS under basal glucose conditions were elevated both *in vivo* and *in vitro*. Despite ameliorated gene expression of *glucokinase*, we could not confirm the obvious elevation of glucokinase protein level. To make clear these points, further studies including glucokinase activity may be needed. HFD-fed Tg mice did not show increased beta cell proliferation (Supplemental Fig. 3D). One possibility is that HFD itself already increased beta cell mass and proliferation to sufficient levels where additional effects were not required to improve beta cell function. These findings suggest that small-Maf factors regulate not only insulin transcription via MARE binding but also possibly intracellular glucose metabolism and insulin release from beta cells via glucokinase expression.

Previous reports on small-Maf factors have already established that they play crucial roles in stress signalling, such as in the case of oxidative stress (17). In terms of the response to stress, small-Maf factors may suppress excessive insulin expression to avoid the accumulation of

370 intracellular endoplasmic reticulum (ER) stress in beta cells presumably via Nrf2, which is one of the
371 counterparts of small Maf factors. Although overexpression of both MafA and DN-MafK results in
372 enhanced insulin gene expression, insulin synthesis, and insulin secretion, but DN-MafK can uniquely
373 accomplish these objectives without enhancing MafA expression.
374 In conclusion, small-Maf factors play important roles as inhibitors of insulin transcription
375 and secretion and, possibly, regulators of intracellular glucose metabolism. Further investigation of
376 the function of endogenous small Maf factors in pancreatic beta cells can lead to a better
377 understanding of the pathogenesis of diabetes.
378

ACKNOWLEDGMENTS

This work was financially supported by grants from the Japanese Ministry of Education, Culture, Sports, Science, Technology Foundation and the Suzuken Memorial Foundation (H.M.) and NIH RO1 DK60127 (A.S.).

No potential conflicts of interest relevant to this article were reported.

H.N. contributed to the experiments and data analysis and wrote the manuscript. A.N. and K.Y. contributed to islet isolation and experiments. H.M. and T.A. contributed to discussion and reviewed and edited the manuscript. A.S. contributed to discussion and reviewed the manuscript. T.K. designed and performed the research and wrote the manuscript. T.K. is the guarantor of this work, has full access to all the data in the study, and takes responsibility for the integrity of the data and accuracy of the data analysis.

Parts of this study were presented at the 74st Scientific Sessions of the American Diabetes Association, San Francisco, California, June 13–17, 2014.

The authors thank Ms. N. Fujimori, Ms. C. Seo, and Ms. M. Watanabe for technical assistance; Dr. Masa-aki Watanabe for contribution to islet isolation. We thank Dr. Yamaoka for providing human insulin promoter construct to T.K. and Dr. Stuart H. Orkin for providing dominant-negative MafK construct to A.S. H.N. and T.K. thank Dr. Nobuaki Ozaki (Nagoya University, Nagoya, Japan) for the helpful discussion.

REFERENCES

1. Olson LK, Redmon JB, Towle HC, Robertson RP. Chronic exposure of HIT cells to high glucose concentrations paradoxically decreases insulin gene transcription and alters binding of insulin gene regulatory protein. The Journal of clinical investigation 1993; 92:514-519
2. Poitout V, Olson LK, Robertson RP. Chronic exposure of betaTC-6 cells to supraphysiologic concentrations of glucose decreases binding of the RIPE3b1 insulin gene transcription activator. The Journal of clinical investigation 1996; 97:1041-1046
3. Sharma A, Olson LK, Robertson RP, Stein R. The reduction of insulin gene transcription in HIT-T15 beta cells chronically exposed to high glucose concentration is associated with the loss of RIPE3b1 and STF-1 transcription factor expression. Molecular endocrinology (Baltimore, Md) 1995; 9:1127-1134
4. Kim JW, You YH, Ham DS, Cho JH, Ko SH, Song KH, Son HY, Suh-Kim H, Lee IK, Yoon KH. Suppression of peroxisome proliferator-activated receptor gamma-coactivator-1alpha normalizes the glucolipotoxicity-induced decreased BETA2/NeuroD gene transcription and improved glucose tolerance in diabetic rats. Endocrinology 2009; 150:4074-4083
5. Naya FJ, Stellrecht CM, Tsai MJ. Tissue-specific regulation of the insulin gene by a novel basic helix-loop-helix transcription factor. Genes Dev 1995; 9:1009-1019
6. Naya FJ, Huang HP, Qiu Y, Mutoh H, DeMayo FJ, Leiter AB, Tsai MJ. Diabetes, defective pancreatic morphogenesis, and abnormal enteroendocrine differentiation in BETA2/neuroD-deficient mice. Genes Dev 1997; 11:2323-2334
7. Kataoka K. MafA Is a Glucose-regulated and Pancreatic beta -Cell-specific Transcriptional Activator for the Insulin Gene. Journal of Biological Chemistry 2002; 277:49903-49910
8. Olbrot M, Rud J, Moss LG, Sharma A. Identification of beta-cell-specific insulin gene transcription factor RIPE3b1 as mammalian MafA. Proc Natl Acad Sci U S A 2002; 99:6737-6742
9. Matsuoka TA, Artner I, Henderson E, Means A, Sander M, Stein R. The MafA transcription factor appears to be responsible for tissue-specific expression of insulin. Proc Natl Acad Sci U S A 2004; 101:2930-2933
10. Kataoka K, Han SI, Shioda S, Hirai M, Nishizawa M, Handa H. MafA is a glucose-regulated and pancreatic beta-cell-specific transcriptional activator for the insulin gene. The Journal of biological chemistry 2002; 277:49903-49910
11. Zhang C, Moriguchi T, Kajihara M, Esaki R, Harada A, Shimohata H, Oishi H, Hamada M, Morito N, Hasegawa K, Kudo T, Engel JD, Yamamoto M, Takahashi S. MafA is a key regulator of glucose-stimulated insulin secretion. Molecular and cellular biology 2005; 25:4969-4976
12. Mears AJ, Kondo M, Swain PK, Takada Y, Bush RA, Saunders TL, Sieving PA, Swaroop A. Nrl is required for rod photoreceptor development. Nat Genet 2001; 29:447-452
13. Blank V, Andrews NC. The Maf transcription factors: regulators of differentiation. Trends

435 Biochem Sci 1997; 22:437-441
436 **14.** Toki T, Itoh J, Kitazawa J, Arai K, Hatakeyama K, Akasaka J, Igarashi K, Nomura N,
437 Yokoyama M, Yamamoto M, Ito E. Human small Maf proteins form heterodimers with CNC
438 family transcription factors and recognize the NF-E2 motif. Oncogene 1997; 14:1901-1910
439 **15.** Shimokawa N, Okada J, Miura M. Cloning of MafG homologue from the rat brain by
440 differential display and its expression after hypercapnic stimulation. Mol Cell Biochem 2000;
441 203:135-141
442 **16.** Kumaki I, Yang D, Koibuchi N, Takayama K. Neuronal expression of nuclear transcription
443 factor MafG in the rat medulla oblongata after baroreceptor stimulation. Life Sci 2006;
444 78:1760-1766
445 **17.** Blank V. Small Maf proteins in mammalian gene control: mere dimerization partners or
446 dynamic transcriptional regulators? Journal of molecular biology 2008; 376:913-925
447 **18.** Kataoka K, Igarashi K, Itoh K, Fujiwara KT, Noda M, Yamamoto M, Nishizawa M. Small
448 Maf proteins heterodimerize with Fos and may act as competitive repressors of the NF-E2
449 transcription factor. Molecular and cellular biology 1995; 15:2180-2190
450 **19.** Shimokawa N, Kumaki I, Qiu CH, Ohmiya Y, Takayama K, Koibuchi N. Extracellular
451 acidification enhances DNA binding activity of MafG-FosB heterodimer. Journal of cellular
452 physiology 2005; 205:77-85
453 **20.** Shimohata H, Yoh K, Morito N, Shimano H, Kudo T, Takahashi S. MafK overexpression in
454 pancreatic beta-cells caused impairment of glucose-stimulated insulin secretion. Biochem
455 Biophys Res Commun 2006; 346:671-680
456 **21.** Kotkow KJ, Orkin SH. Dependence of globin gene expression in mouse erythroleukemia cells
457 on the NF-E2 heterodimer. Molecular and cellular biology 1995; 15:4640-4647
458 **22.** Hino S, Yamaoka T, Yamashita Y, Yamada T, Hata J, Itakura M. In vivo proliferation of
459 differentiated pancreatic islet beta cells in transgenic mice expressing mutated
460 cyclin-dependent kinase 4. Diabetologia 2004; 47:1819-1830
461 **23.** Nakamura A, Togashi Y, Orime K, Sato K, Shirakawa J, Ohsugi M, Kubota N, Kadowaki T,
462 Terauchi Y. Control of beta cell function and proliferation in mice stimulated by
463 small-molecule glucokinase activator under various conditions. Diabetologia 2012;
464 55:1745-1754
465 **24.** Watanabe M, Yamashita K, Kamachi H, Kuraya D, Koshizuka Y, Shibasaki S, Asahi Y, Ono H,
466 Emoto S, Ogura M, Yoshida T, Ozaki M, Umezawa K, Matsushita M, Todo S. Efficacy of
467 DHMEQ, a NF-kappaB inhibitor, in islet transplantation: II. Induction DHMEQ treatment
468 ameliorates subsequent alloimmune responses and permits long-term islet allograft
469 acceptance. Transplantation 2013; 96:454-462
470 **25.** Panakanti R, Mahato RI. Bipartite vector encoding hVEGF and hIL-1Ra for ex vivo
471 transduction into human islets. Molecular pharmaceutics 2009; 6:274-284
472 **26.** Shimohata H, Yoh K, Fujita A, Morito N, Ojima M, Tanaka H, Hirayama K, Kobayashi M,

Kudo T, Yamagata K, Takahashi S. MafA-deficient and beta cell-specific MafK-overexpressing hybrid transgenic mice develop human-like severe diabetic nephropathy. Biochem Biophys Res Commun 2009; 389:235-240

27. Ferre T, Riu E, Bosch F, Valera A. Evidence from transgenic mice that glucokinase is rate limiting for glucose utilization in the liver. FASEB J 1996; 10:1213-1218

28. Matschinsky FM. Assessing the potential of glucokinase activators in diabetes therapy. Nat Rev Drug Discov 2009; 8:399-416

29. Froguel P, Zouali H, Vionnet N, Velho G, Vaxillaire M, Sun F, Lesage S, Stoffel M, Takeda J, Passa P, et al. Familial hyperglycemia due to mutations in glucokinase. Definition of a subtype of diabetes mellitus. The New England journal of medicine 1993; 328:697-702

30. Nakamura A, Terauchi Y, Ohyama S, Kubota J, Shimazaki H, Nambu T, Takamoto I, Kubota N, Eiki J, Yoshioka N, Kadowaki T, Koike T. Impact of small-molecule glucokinase activator on glucose metabolism and beta-cell mass. Endocrinology 2009; 150:1147-1154

31. Terauchi Y, Takamoto I, Kubota N, Matsui J, Suzuki R, Komeda K, Hara A, Toyoda Y, Miwa I, Aizawa S, Tsutsumi S, Tsubamoto Y, Hashimoto S, Eto K, Nakamura A, Noda M, Tobe K, Aburatani H, Nagai R, Kadowaki T. Glucokinase and IRS-2 are required for compensatory beta cell hyperplasia in response to high-fat diet-induced insulin resistance. The Journal of clinical investigation 2007; 117:246-257

32. Wang H, Brun T, Kataoka K, Sharma AJ, Wollheim CB. MAFA controls genes implicated in insulin biosynthesis and secretion. Diabetologia 2007; 50:348-358

33. Aguayo-Mazzucato C, Koh A, El Khattabi I, Li WC, Toschi E, Jermendy A, Juhl K, Mao K, Weir GC, Sharma A, Bonner-Weir S. Mafa expression enhances glucose-responsive insulin secretion in neonatal rat beta cells. Diabetologia 2011; 54:583-593

34. Moates JM, Nanda S, Cissell MA, Tsai MJ, Stein R. BETA2 activates transcription from the upstream glucokinase gene promoter in islet beta-cells and gut endocrine cells. Diabetes 2003; 52:403-408

501 **FIGURES AND LEGENDS**

502

503 **Figure 1.** Enhanced small-Maf expression in pancreatic beta cells in C57BL/6J mice fed a high-fat
504 diet (HFD).
505 A: MafF/G/K and Actin expression in 3 independent experimental islets isolated from 12-week-old
506 mice fed a normal diet (ND) or an HFD are detected by Western blotting. Quantitation of band density
507 was performed using an imaging densitometer. Values are expressed as mean ± standard error. *$p <$
508 0.05.
509 B: Representative images of MafF/G/K and insulin staining in islets from ND- and HFD-fed mice.
510 MafF/G/K proteins are detected in the nuclei of pancreatic beta cells from each mouse using an
511 anti-MafF/G/K antibody.
512 C: Immunohistochemistry of beta cells per high power field (Green: insulin, Red: MafF/G/K, Blue:
513 DAPI). MafF/G/K expression is confirmed mostly in the nuclei of beta cells.

514

515 **Figure 2.** Studies of adenovirus (Ad)-infected MIN6 cells.
516 A: Confirmation of multiplicity of adenovirus infection. We selected multiplicity of infection of
517 roughly 20, and infection were confirmed almost all MIN6 cells.
518 B: Confirmation of dominant-negative MafK (DN-MafK) expression of Ad-DN-MafK–infected
519 MIN6 cells. Band (a) and (b) indicate Flag-DN-MafK, endogenous MafF/G/K, respectively.
520 MafF/G/K antibody, Flag antibody, and Actin antibody are presented.

521

522 **Figure 3.** Characteristics of DN-MafK construct.
523 A: Schematic image of DN-MafK lacking basic regions in the DNA-binding domain.
524 B: DNA-binding activity to the Maf recognition element (MARE) on the insulin promoter 2 using a
525 chromatin immunoprecipitation (ChIP) assay using MIN6 cells (n = 6).
526 Quantitation of relative band density compared with IgG bands is performed using an imaging
527 densitometer. White bars = Control adenovirus (Ad-GFP)-infected MIN6 cells, Black bars =

adenovirus dominant-negative MafK (Ad-DN-MafK)-infected MIN6 cells. Values are expressed as means ± standard errors. *$p < 0.05$ and **$p < 0.01$.

C: Relative insulin promoter transcriptional activity using a luciferase assay. White bars =Ad-GFP-infected MIN6 cells, Black bars = Ad-DN-MafK-infected MIN6 cells. Values are expressed as means ± standard errors. ***$p < 0.001$.

Figure 4. Generation of transgenic mice with beta cell–specific expression of dominant-negative MafK (DN-MafK) established on a C57BL/6J background.

A: Copy numbers of the integrated transgene in lines No. 72, 23, and 53 of the transgenic (Tg) mice as determined by Southern blotting.

B: DN-MafK expression in various tissues as analysed by Western blotting

(**1**: brain, **2**: heart, **3**: lung, **4**: liver, **5**: spleen, **6**: pancreas, **7**: kidney, **8**: intestine, **9**: fat)

Flag-DN-MafK is detected only in the pancreas.

C: Representative images of Flag-DN-MafK staining in islets in wild-type (Wt) and Tg mice

Flag-DN-MafK is co-stained with insulin-positive cells in the Tg mice.

D, E: Intraperitoneal glucose tolerance tests were conducted at 20 weeks of age (n = 6–10). The Tg mice show a significant improvement in blood glucose (D) and augmentation of early phase insulin secretion (E) compared with the Wt mice only under the high-fat diet (HFD) condition. Black circles = Wt mice on a normal diet (ND), white circles = Wt mice on a HFD, black squares = DN-MafK Tg mice on a ND, white squares = DN-MafK Tg mice on a HFD.

F: DN-MafK and MafA expression in isolated islets from the ND-fed or HFD-fed Wt and Tg mice as detected by Western blotting. Actin is used as a loading control. MafA is similarly elevated under the HFD condition in both the Wt and Tg mice.

Figure 5. Metabolism of wild-type (Wt) and dominant-negative MafK (DN-MafK) transgenic (Tg) mice under the high-fat diet (HFD) condition.

A, B: Body weight (A) and ad libitum-fed blood glucose levels (B) are measured in the Wt mice

555 (white circles) and DN-MafK Tg mice (black circles) at 6–16 weeks of age (n = 18–21). Body weight
556 is not different between the Wt and Tg mice, while blood glucose levels are lower in the Tg mice.
557 C, D: The intraperitoneal insulin tolerance test (C) and oral glucose tolerance test (OGTT) (D) are
558 performed in the Wt mice (white circles) and DN-MafK Tg mice (black circles) at 16–17 weeks of
559 age (n = 9–10, n = 14–17, respectively). While insulin sensitivity is not different, glucose tolerance is
560 significantly improved in the DN-MafK Tg mice.
561 E: Area under the glucose curve (AUC) during the OGTT in the HFD-fed mice (n = 14–17). The AUC
562 was also significantly lower in the Tg mice.
563 F: Serum insulin concentrations are measured during OGTT (n = 10 for each group). The Tg mice
564 show high levels of serum insulin both before and after glucose loading. Values are expressed as
565 means ± standard errors. ***$p < 0.001$.
566
567 **Figure 6**. Glucose-stimulated insulin secretion assay of mouse isolated islets.
568 A, B: Glucose-stimulated insulin secretion using size-matching isolated islets. After pre-incubation
569 with Krebs–Ringer bicarbonate HEPES (KRBH) buffer containing 2.8 mM glucose for 30 min, the
570 islets are incubated in the presence of 2.8, 5.6 and 11.2 mM glucose for 90 min. Supernatant insulin
571 concentration is measured (A). (B) shows insulin concentration adjusted for insulin content of each
572 well. [n = 4 for each group, wild-type (Wt) mice = white bars, transgenic (Tg) mice = black bars].
573 C: The insulin content in pancreatic islets is determined after acid-ethanol extraction. The islets from
574 the Tg mice contained high insulin levels (n = 20, Wt = white bars, Tg = black bars).
575
576 **Figure 7**. Gene expressions of isolated islets and Ad-infected MIN6.
577 A: Comparison of gene expression between the Wt islets (white bars) and dominant-negative MafK
578 (DN-MafK) Tg islets (black bars; n = 4 for each group). *Insulin1, insulin2, and glucokinase* were
579 significantly elevated in the HFD-fed Tg mice compared with those in the Wt mice (n = 4 for each
580 group, Wt = white bars, Tg = black bars). Values are expressed as means ± standard errors. **$p <$
581 0.01.

582 B: Comparison of gene expression between control adenovirus (Ad-GFP; white bars) and adenovirus
583 dominant-negative MafK (Ad-DN-MafK; black bars)-infected MIN6 cells (n = 6 for each group).
584 DN-MafK expression significantly elevated *insulin1* and *insulin2* and tended to increase *glucokinase*
585 (n = 6 for each group). Values are expressed as means ± standard errors. *$p < 0.05$.
586

Fig 1.

A

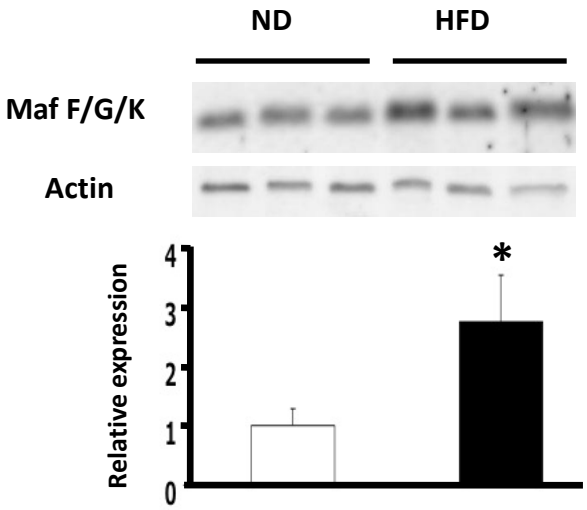
ND
HFD
Maf F/G/K
Actin
Relative expression
0
1
2
3
4
*

B

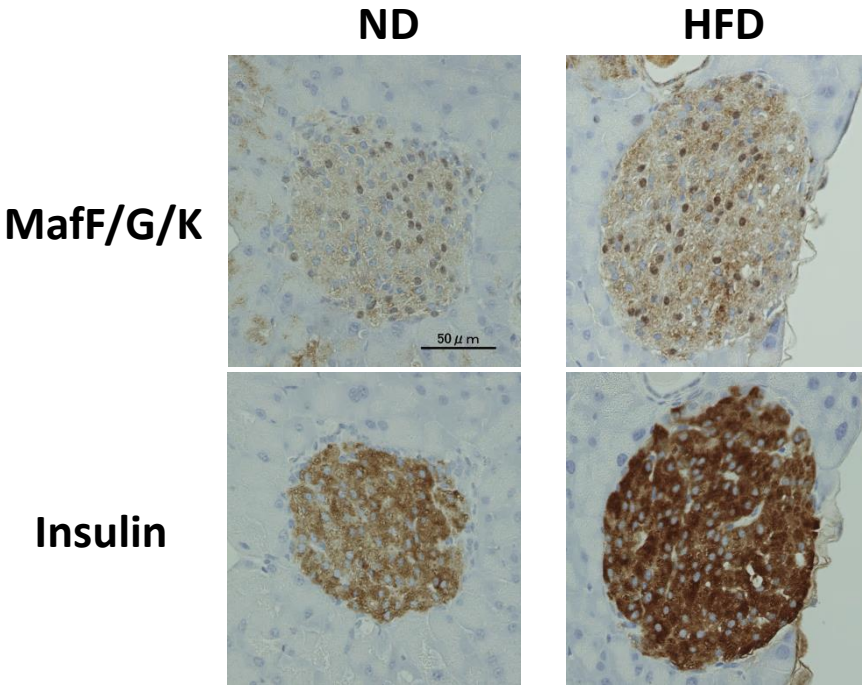
ND
HFD
MafF/G/K
Insulin
50 μm

C

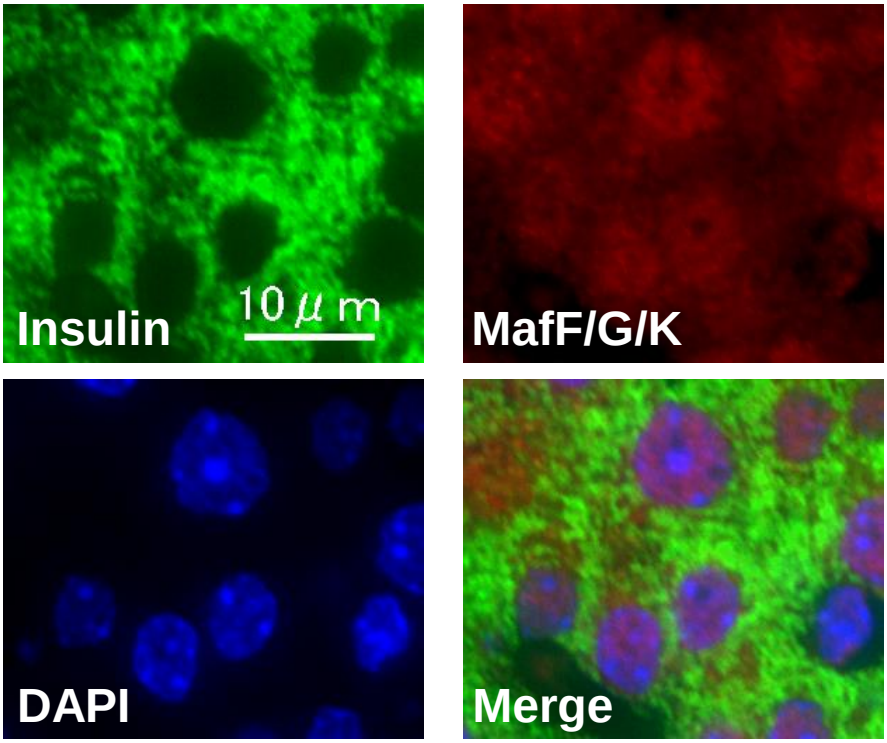
Insulin
10 μm
MafF/G/K
DAPI
Merge

Fig 2.

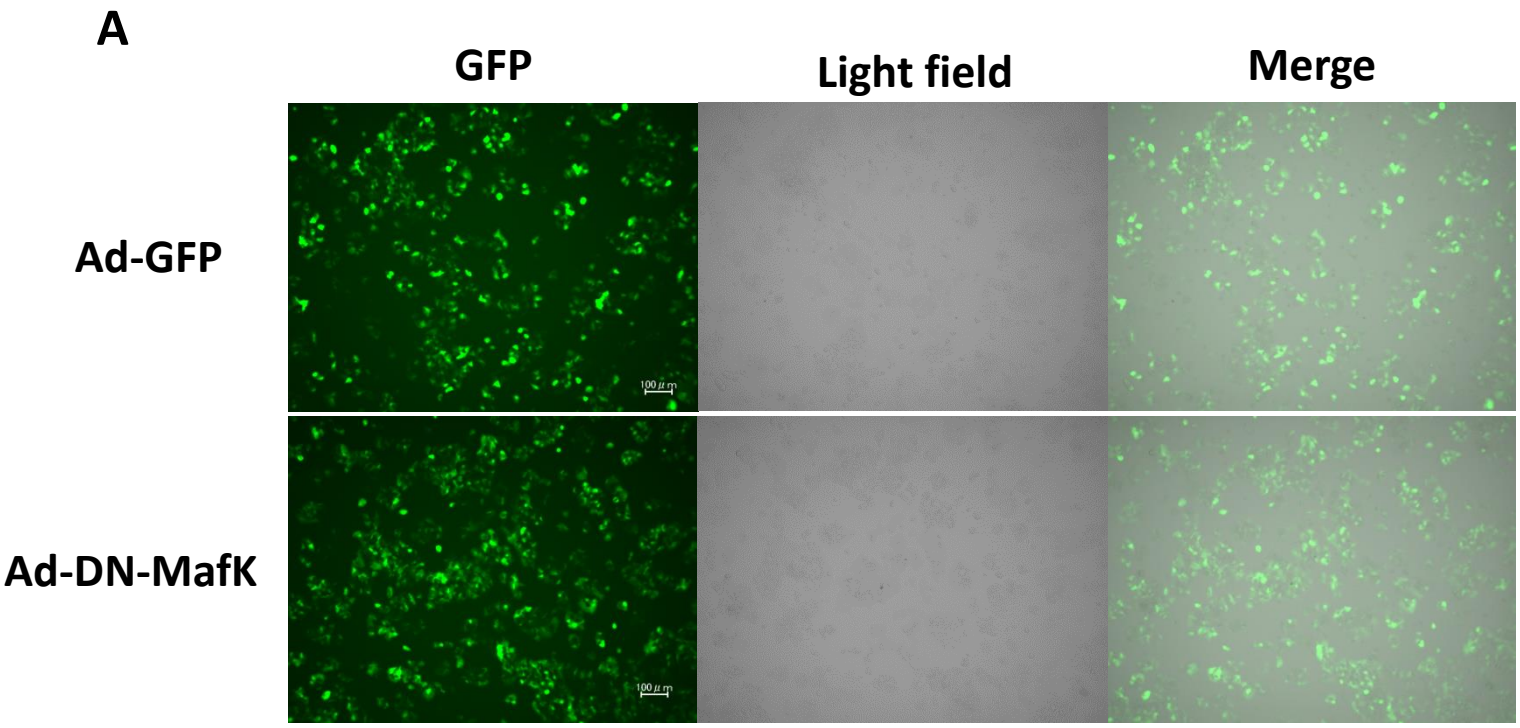
A
GFP
Light field
Merge
Ad-GFP
Ad-DN-MafK

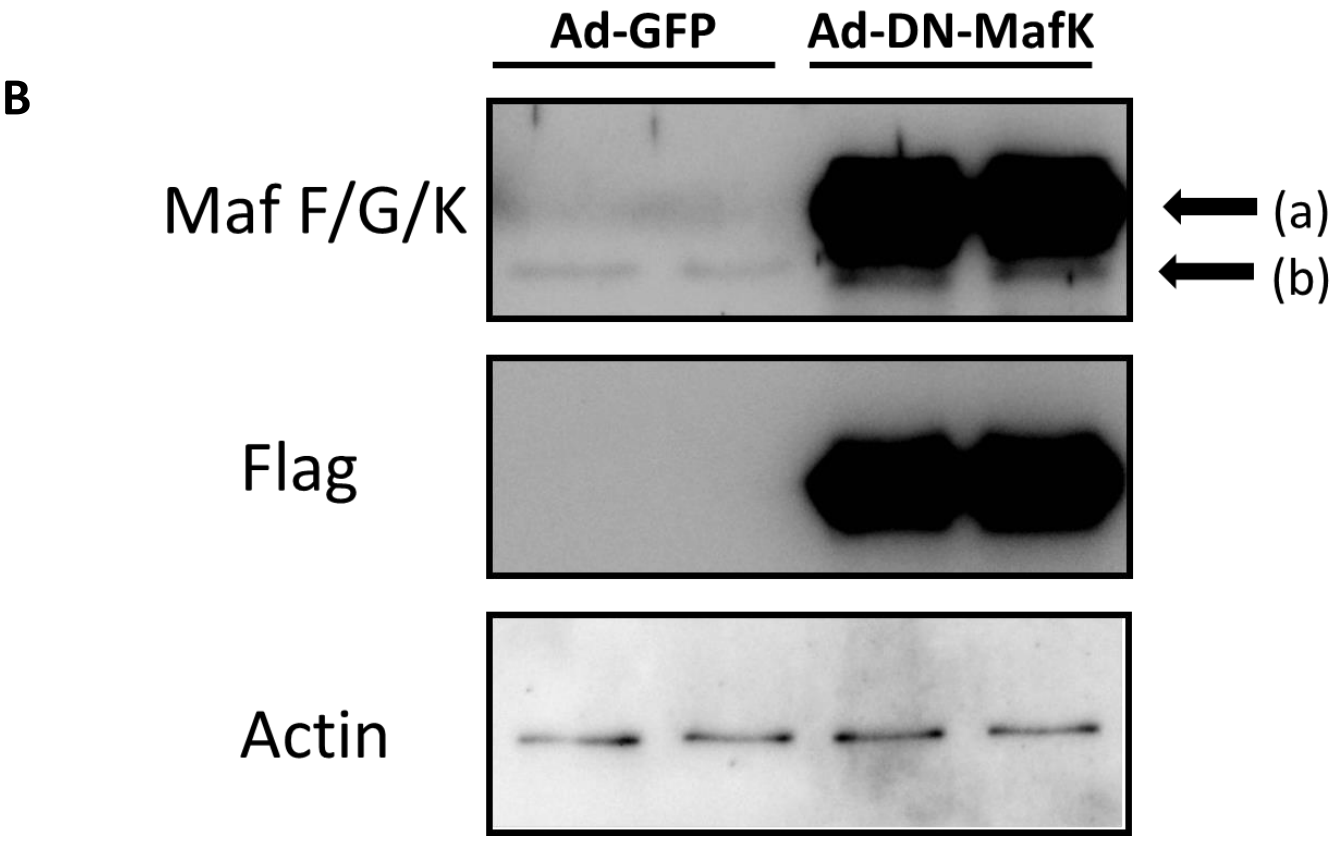
B
Ad-GFP
Ad-DN-MafK
Maf F/G/K
(a)
(b)
Flag
Actin

Fig 3.

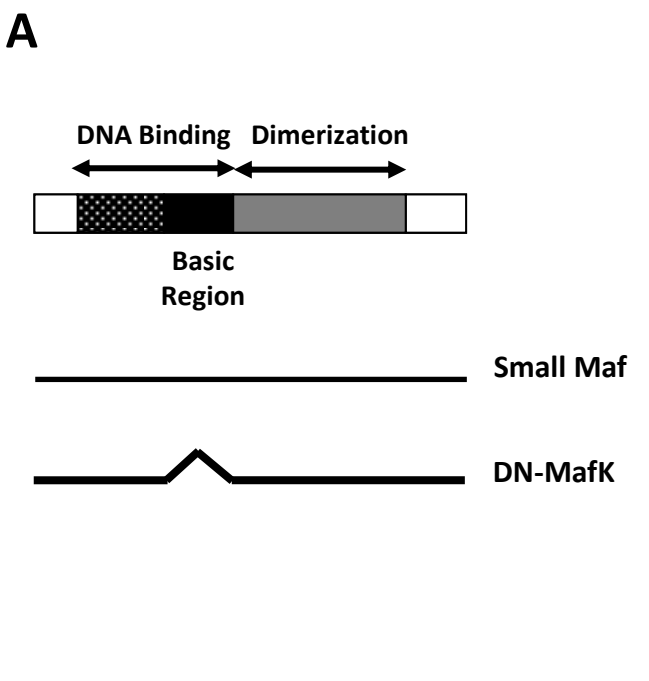
A
DNA Binding
Dimerization
Basic
Region
Small Maf
DN-MafK

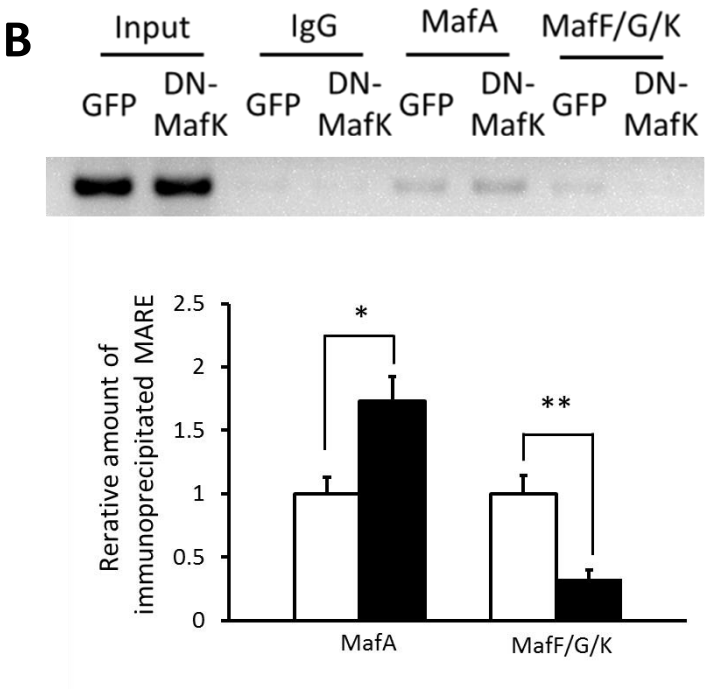
B
Input
IgG
MafA
MafF/G/K
GFP
DN-MafK
GFP
DN-MafK
GFP
DN-MafK
GFP
DN-MafK
Rerative amount of immunoprecipitated MARE
2.5
2
1.5
1
0.5
0
*
**
MafA
MafF/G/K

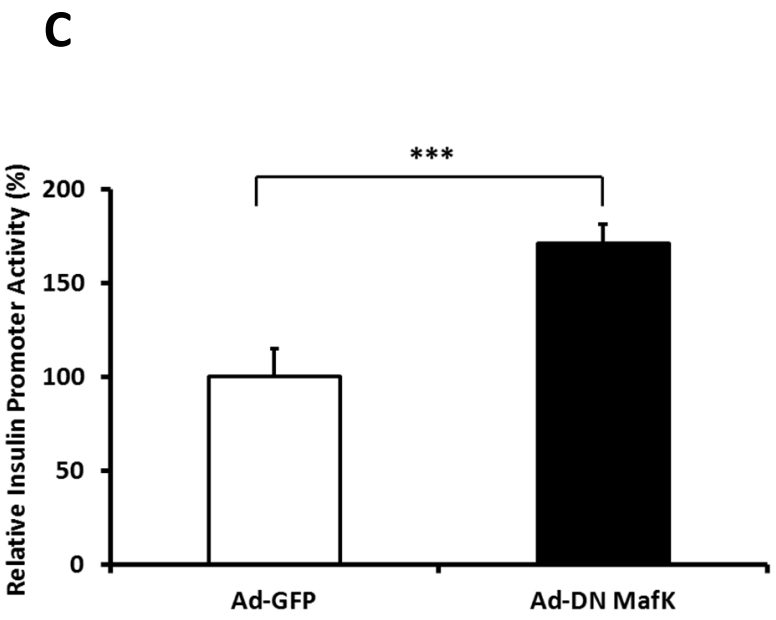
C
***
Relative Insulin Promoter Activity (%)
200
150
100
50
0
Ad-GFP
Ad-DN MafK

Fig 4.

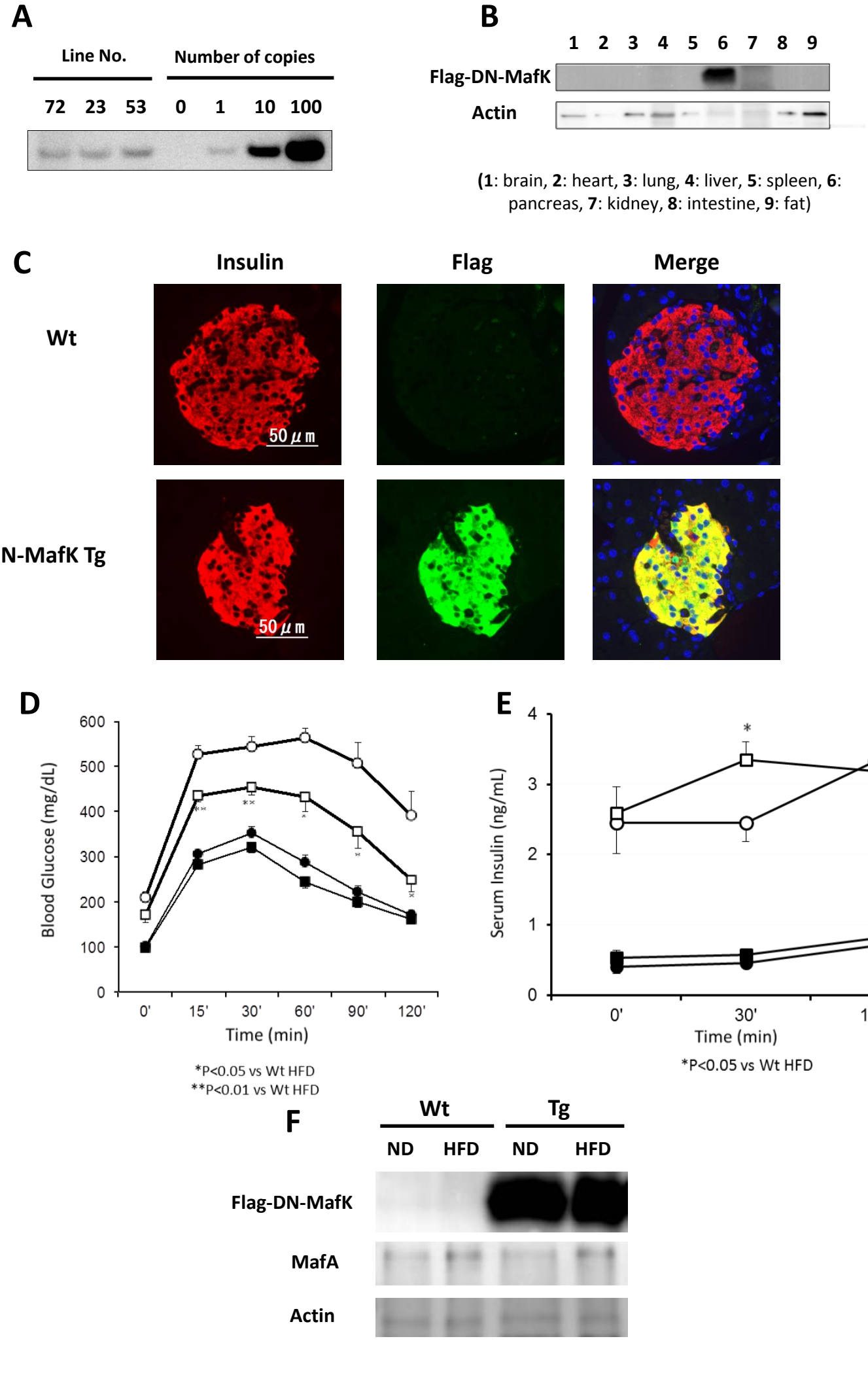
A
Line No.
Number of copies
72 23 53 0 1 10 100
B
1 2 3 4 5 6 7 8 9
Flag-DN-MafK
Actin
(1: brain, 2: heart, 3: lung, 4: liver, 5: spleen, 6: pancreas, 7: kidney, 8: intestine, 9: fat)
C
Insulin
Flag
Merge
Wt
DN-MafK Tg
50 μm
50 μm
D
Blood Glucose (mg/dL)
600
500
400
300
200
100
0
0' 15' 30' 60' 90' 120'
Time (min)
*P<0.05 vs Wt HFD
**P<0.01 vs Wt HFD
E
Serum Insulin (ng/mL)
4
3
2
1
0
0' 30' 120'
Time (min)
*P<0.05 vs Wt HFD
F
Wt
Tg
ND HFD ND HFD
Flag-DN-MafK
MafA
Actin

Fig 5.

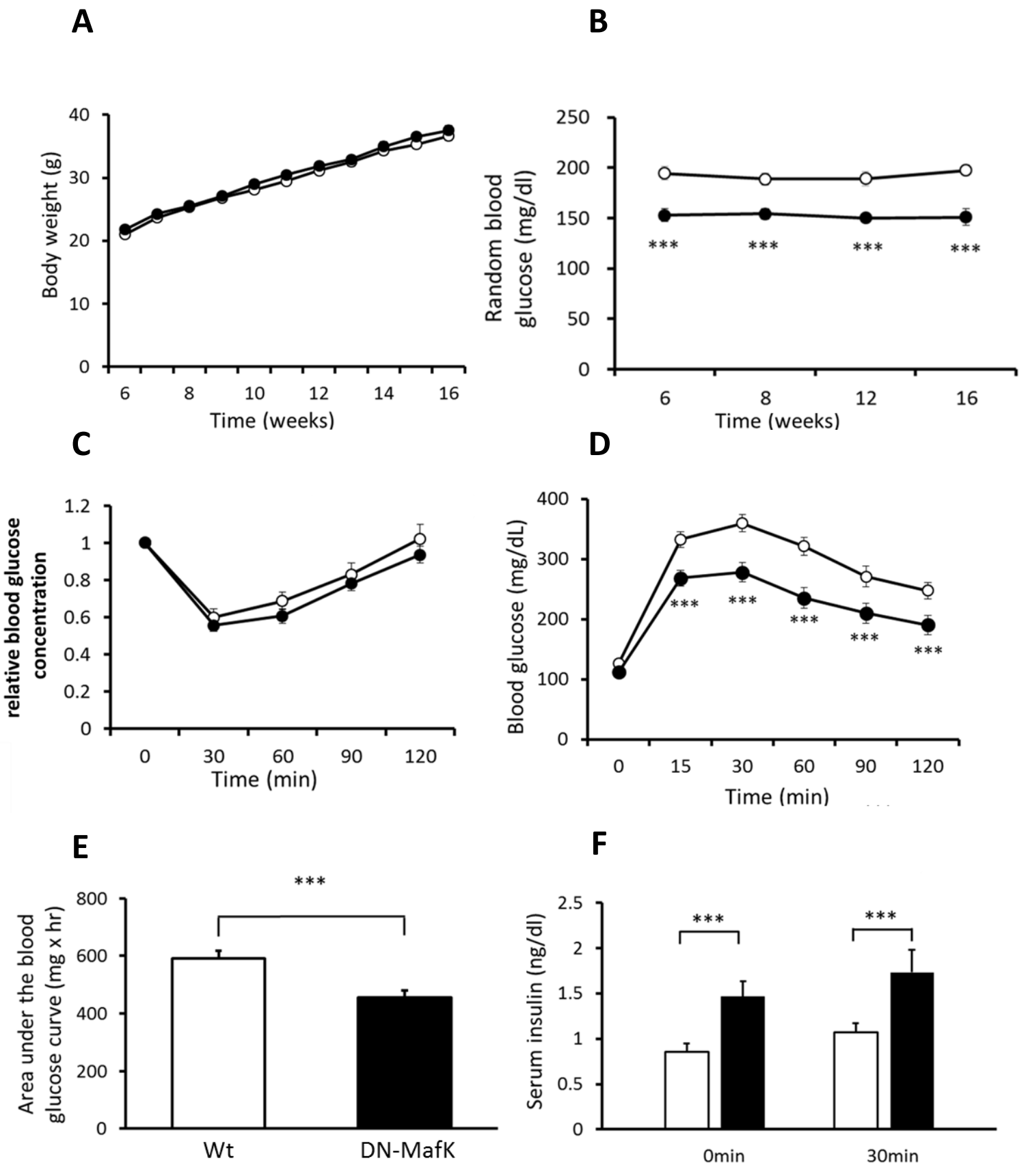
A
Body weight (g)
40
30
20
10
0
6
8
10
12
14
16
Time (weeks)
B
Random blood glucose (mg/dl)
250
200
150
100
50
0
***
***
***
***
6
8
12
16
Time (weeks)
C
relative blood glucose concentration
1.2
1
0.8
0.6
0.4
0.2
0
0
30
60
90
120
Time (min)
D
Blood glucose (mg/dL)
400
300
200
100
0
***
***
***
***
***
0
15
30
60
90
120
Time (min)
E
***
Area under the blood glucose curve (mg x hr)
800
600
400
200
0
Wt
DN-MafK
F
Serum insulin (ng/dl)
2.5
2
1.5
1
0.5
0
***
***
0min
30min

Fig 6.

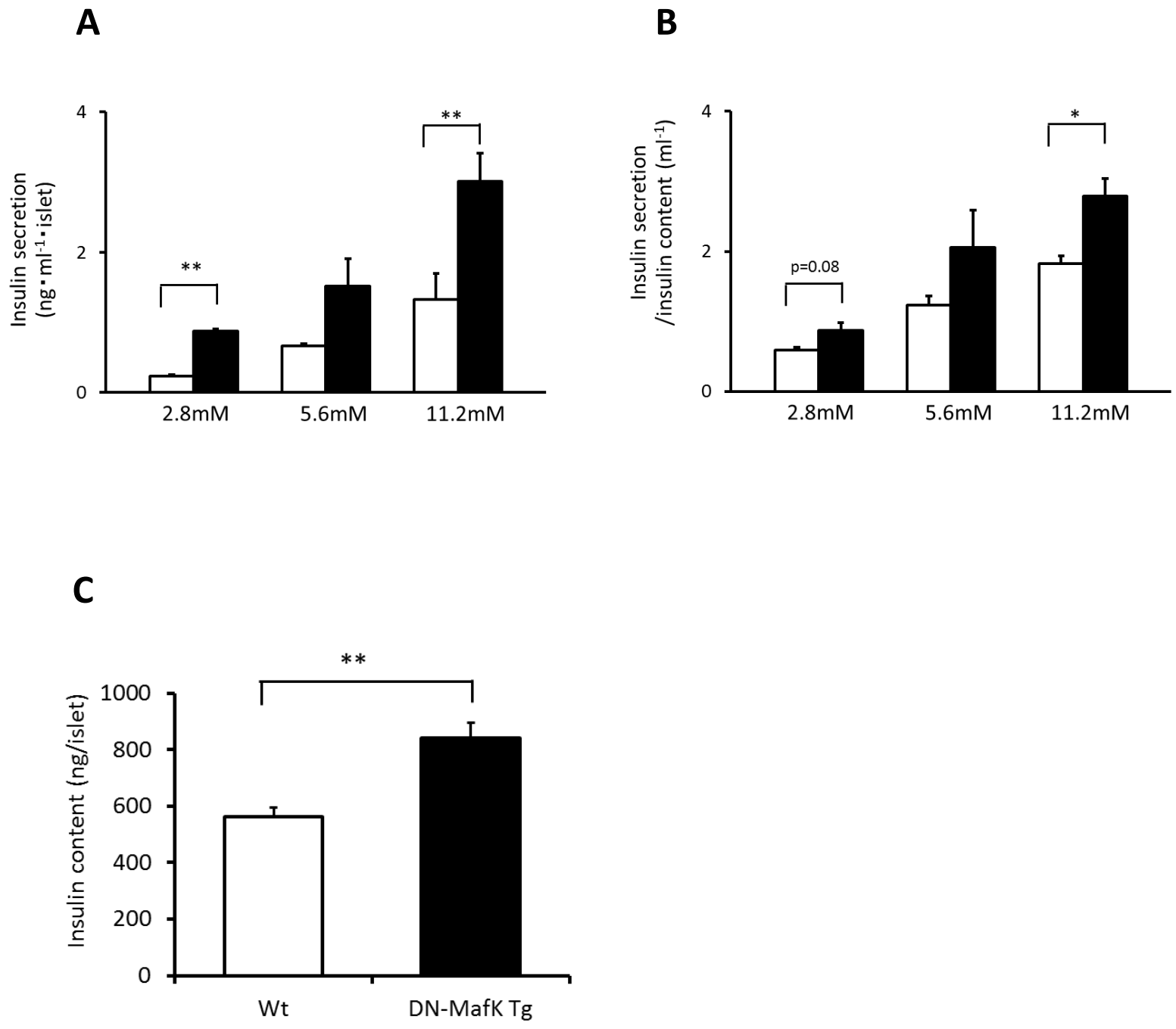
A
Insulin secretion
(ng・ml-1・islet)
4
2
0
**
**
2.8mM
5.6mM
11.2mM
B
Insulin secretion
/insulin content (ml-1)
4
2
0
p=0.08
*
2.8mM
5.6mM
11.2mM
C
Insulin content (ng/islet)
1000
800
600
400
200
0
**
Wt
DN-MafK Tg

Fig 7.

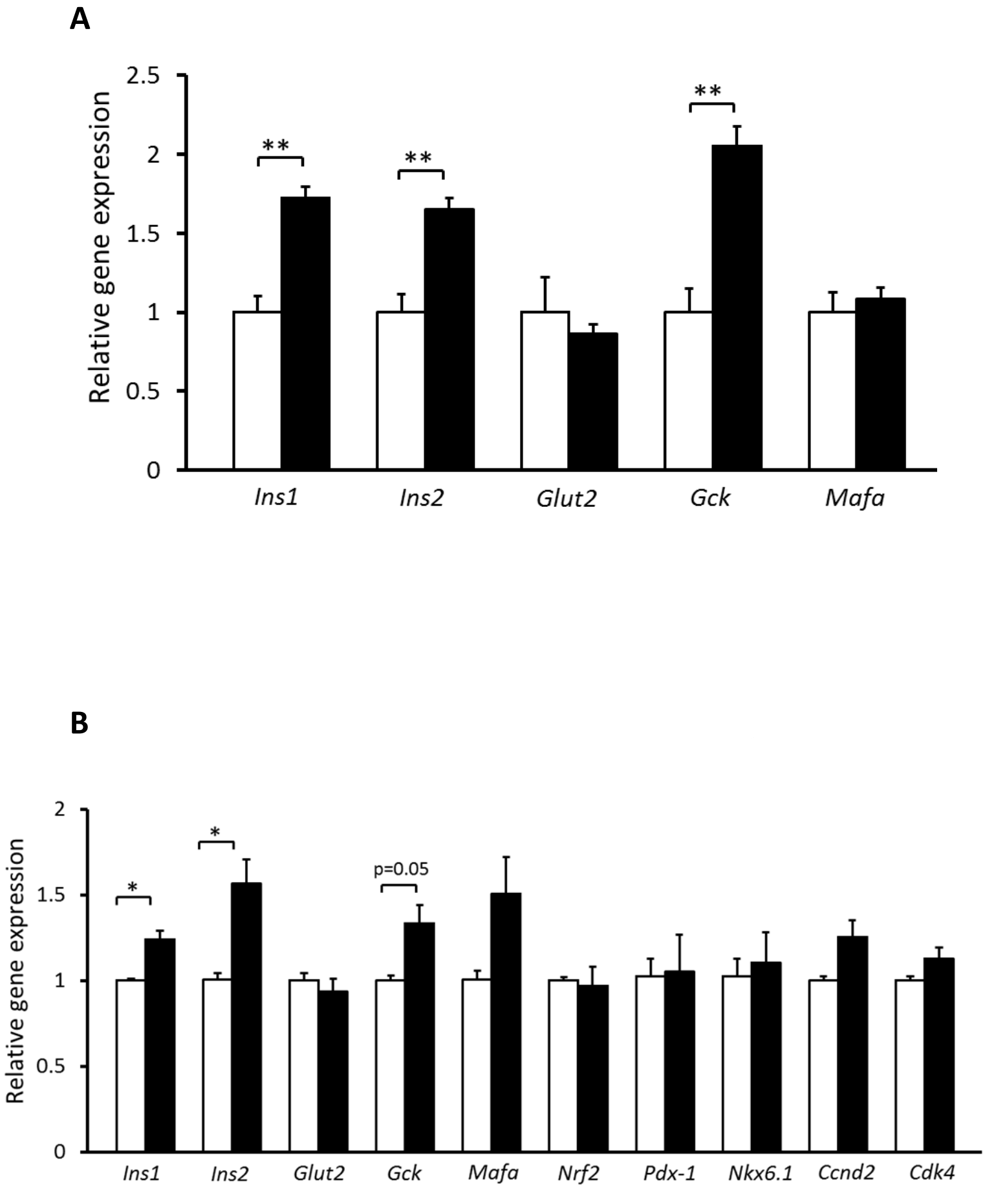
A
Relative gene expression
2.5
2
1.5
1
0.5
0
**
**
**
Ins1
Ins2
Glut2
Gck
Mafa
B
Relative gene expression
2
1.5
1
0.5
0
*
*
p=0.05
Ins1
Ins2
Glut2
Gck
Mafa
Nrf2
Pdx-1
Nkx6.1
Ccnd2
Cdk4